ELSEVIER

Materials Science and Engineering A 447 (2007) 192–196

MATERIALS SCIENCE & ENGINEERING A

www.elsevier.com/locate/msea

Effect of pre/post T6 heat treatment on the mechanical properties of laser welded SSM cast A356 aluminium alloy

R. Akhter[a,*], L. Ivanchev[b], H.P. Burger[a]

[a] CSIR, National Laser Centre, P.O. Box 395, Pretoria 0001, South Africa

[b] CSIR, Materials Science and Manufacturing, P.O. Box 395, Pretoria 0001, South Africa

Received 5 June 2006; received in revised form 10 September 2006; accepted 26 October 2006

Abstract

Aluminium alloy A356 was treated by the Rheo semi solid metal (SSM) process, developed recently by CSIR-Pretoria, and cast in plates using a high pressure die casting (HPDC) machine. Plates in as cast condition (F) and heat treated T6 condition (pre HT) were butt welded, using an Nd:YAG laser. In another experiment, as cast welded samples were heat treated to T6 condition (post HT). The base metal and weld microstructures were presented. The effect of heat treatments on microstructure and mechanical properties of the welds was investigated. It was found that the fine dendrite structure of the weld metal contributed to the mechanical properties of the joint. The mechanical properties of the post HT samples were found to be higher than the pre HT and as cast materials.

Keywords: Laser; Welding; Aluminium; Alloys; SSM cast A356; Semi solid metals; HPDC; Heat treatment

1. Introduction

There are two types of semi solid forming technologies available at present, Rheo and Thixo casting. Rheo casting involves the preparation of SSM slurry directly from liquid alloys by stirring during solidification and casting the slurry with a HPDC machine directly into a die for component manufacturing. Thixo casting is a two step process, which involves the preparation of a feedstock material with thixotropic characteristic (globular microstructure), and reheating of the material to semi solid temperature to produce SSM slurry to be used to form components [1,2].

Laser welding is widely used in industrial production owing to the advantages such as low heat input, high welding speed, high production rate, etc. [3,4]. The automobile industries are increasing the use of aluminium alloys because of the greater demand for lightweight and high strength materials resulting in reduced fuel consumption. Welding of aluminium alloys poses many problems like porosities, blowholes and cracks in the weld bead [5]. Due to the unique processing advantages offered by laser welding, the technique is used to weld SSM cast aluminium A356 alloy with the aim of producing a weld seams with acceptable properties.

The purpose of this work is to evaluate the effect that laser welding has on the mechanical properties of the SSM A356 alloy in as cast (F) and heat treated T6 condition. The alloy A356 was chosen because it is commonly used in many automotive components, such as suspension, driveline, and engine parts, where increased durability and reliability are always desirable [6]. Microstructure, hardness and tensile properties of the weld joint have been studied and the results are reported.

2. Materials and methods

The SSM A356 aluminium plates (4 mm × 80 mm × 100 mm) were cast in steel moulds with a 50 tonnes HPDC machine. The CSIR rheo-process and equipment were applied for the treatment of liquid metal to semi solid temperature [7]. The welding was performed using a 4.4 kW Rofin Sinar DY 044 Nd:YAG laser that employed a HIGHYAG ASK welding head mounted on a KUKA KR60L30HA robot. A 600-μm fibre was used for beam delivery. The beam was focused onto the work piece by a lens of 200 mm focal length. The final spot size at the work piece was 0.6 mm. A twin spot configuration was used

* Corresponding author. Tel.: +27 128412147; fax: +27 128413152.
E-mail addresses: RAkhter@csir.co.za, rehan_akhter@hotmail.com (R. Akhter), LIvanch@csir.co.za (L. Ivanchev), HBurger@csir.co.za (H.P. Burger).

0921-5093/$ – see front matter © 2006 Elsevier B.V. All rights reserved.
doi:10.1016/j.msea.2006.10.148

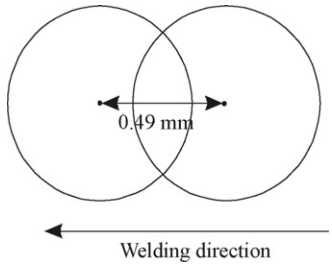

Fig. 1. Configuration of twin spots.

with the twin spots orientated in line with welding direction. The centre-to-centre distance between the twin spots was 0.49 mm. The spot configuration is shown in Fig. 1. The use of dual beam conditions ensures a larger weld pool, facilitates the porosity's ejection and stabilizes the keyhole as compared with single beam configurations.

For each weld the specimen was clamped on a fixed table and the focused beam was moved over the sheet. A shielding gas mixture of argon and helium in the ratio of 2:1 was used during the welding process. This provided an inert shield over the hot reactive weld. The gas flow rate was 20 l/min. Helium is considered to be a good shielding gas in laser welding because high ionisation potential offers resistance to the formation of plasma. Helium is however lighter than air and substantial flow rates are required to produce adequate shielding. Argon on the other hand is heavier than air and provides better shielding. It is however more prone to plasma formation and because it is much heavier than helium it transfers more momentum to the weld pool. In the case of aluminium the weld metal has low viscosity and is easily disturbed. We believed that a mixture of helium and argon would strike an optimum compromise between the requirements of plasma prevention, shielding and the sensitivity of the low viscosity melt pool to mechanical disturbance.

The welding speed was varied for each experimental weld. After the welding process, the welded specimen were sectioned, ground and polished. The weld microstructure was observed by optical microscopy after etching with Keller's solution. X-ray analyses were also performed through out the length of the weld to investigate the presence of porosities. A micro-hardness tester was used to measure the hardness. The tensile tests were performed on a Lloyd M100K machine.

3. Heat treatment

To obtain the T6 heat treatment condition, the as cast and welded samples were solution treated at 540 °C for 6 h and then water quenched before artificially aged at 160 °C for 6 h.

4. Results and discussions

4.1. Laser welding

Laser welding of the SSM A356 aluminium alloy was performed. A range of welding parameters was used for the bead on plate welding. Fig. 2 shows the relationship between welding speed and depth/width of the weld in SSM aluminium. Generally

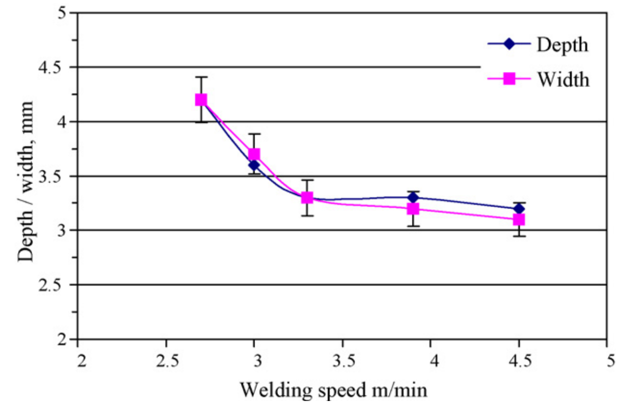

Fig. 2. Welding speed vs. depth/width for welding SSM aluminium A356, laser power 4 kW, sheet thickness 4.2 mm, spot separation 0.49 mm.

the depth and width decreases as the welding speed is increased. It is customary to define the width of the weld as the widest part of the weld metal. This normally occurs at the weld face, i.e. top surface of the substrate. It is generally accepted that the width of the weld increases as the heat input increases. This is often the case when the available laser power is not quite sufficient to give the required penetration and speed has to be reduced in order to ensure full penetration. We believe that this is the reason for the relatively wide welds. Because of the fact that a 600-μm fibre was used the power density was too low for full penetration at high speed. Full penetration could only be obtained at a speed that corresponded to a heat input that was too high. Fig. 3 shows a weld profile made by joining two sheets in butt configuration using optimal parameters.

The composition of the base and weld metals are given in Table 1. It can be seen that there is not a significant change in the composition after welding.

4.2. Microstructure

The microstructure of the as cast (F) base metal and weld fusion zone is shown in Fig. 4a and b. The microstructure of the

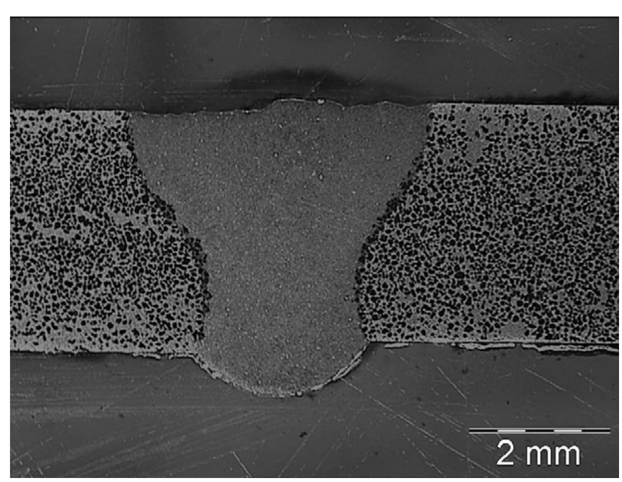

Fig. 3. Weld profile of aluminium alloy in butt configuration: laser power, 3.8 kW; speed, 1.92 m/min; spot separation, 0.49 mm; sheet thickness, 4.0 mm.

Table 1
Percentage composition of the weld

Sample	Element									
	Al	Si	Mg	Fe	Ti	Cu	Mn	Cr	Ni	Sr
Base metal	Balance	7.23	0.38	0.16	0.107	≤0.005	≤0.005	≤0.005	≤0.005	0.039
Weld metal	Balance	7.10	0.36	0.15	0.105	≤0.01	≤0.005	≤0.005	≤0.005	0.025

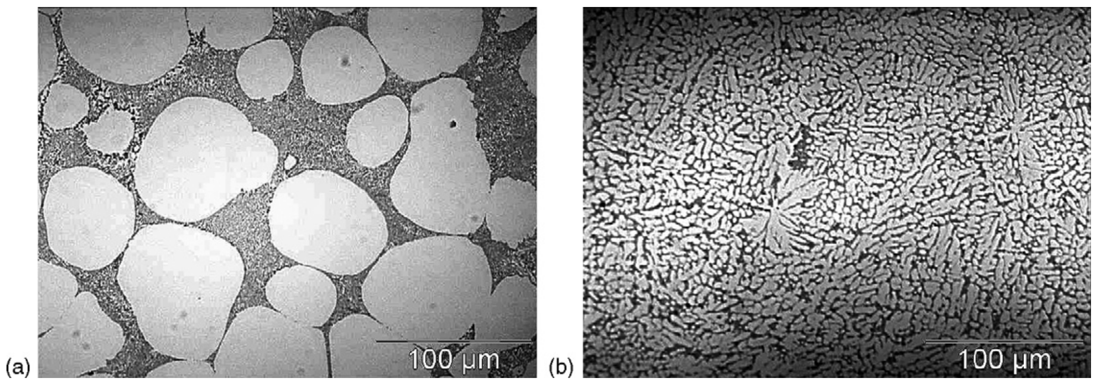

Fig. 4. Microstructure of as cast SSM A356 aluminium: (a) base metal and (b) fusion zone.

base metal consists of primary phase α-Al and a eutectic mixture of Al and Si. The α-Al phases are globular with average grain size of 90 µm. The eutectic of the A356 is also characterised by phases containing Si, Fe and Mg. The shape of these constituents is elongated and irregular as in a typical eutectic structure. The weld fusion zone (Fig. 4b) consists of a finer dendrite structure, due to high cooling rate during solidification. The dendrite length ranges from 10 to 15 µm. The α-Al solidifies as fine dendrites while the eutectic solidified between the dendrite arm spacing.

Fig. 5 shows the microstructure of A356 aluminium alloy pre heat treated (HT) to T6 condition. The base metal consists of α-Al globule. The irregular eutectic of the as cast material was converted into spherodized Si particles due to the solution treatment [8]. The fusion zone of the pre HT, shown in Fig. 5b, was similar in appearance to the fusion zone of the as cast material (Fig. 4b).

Fig. 6 shows the base metal and fusion zone of the post HT weld. The base metal consists of α-Al globule and the Al–Si eutectic with spherodized Si particle. In the fusion zone, the fine dendrite eutectic structure of the as cast weld was also converted into fine globular Si particles uniformly distributed in the Al matrix. Due to the presence of very fine eutectic in the fusion zone, the particle size of the Si (2 µm) was smaller than the base metal Si (4 µm).

4.3. Hardness measurement

The micro-hardness was measured across the weld using a load of 100 g. The results for as cast, pre HT and post HT samples are shown in Fig. 7. The hardness measurements were extended to 6 mm on each side of the weld to include the base metal, which was not affected by the fusion heat. In the case of the as cast conditions, the base metal showed an average hardness of 70 Hv, while the hardness of the weld metal was 90 Hv. The increase in hardness in the weld metal is attributed to the fine dendrite structure of the weld fusion zone.

In the case of welds, which were pre HT, the average hardness of the fusion zone was 95 Hv, which was slightly

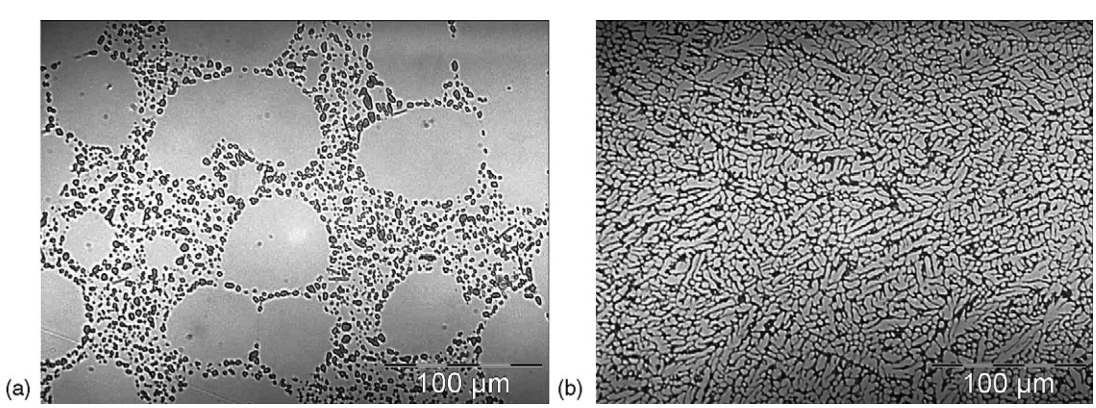

Fig. 5. Microstructure of pre HT A356 aluminium: (a) base metal and (b) fusion zone.

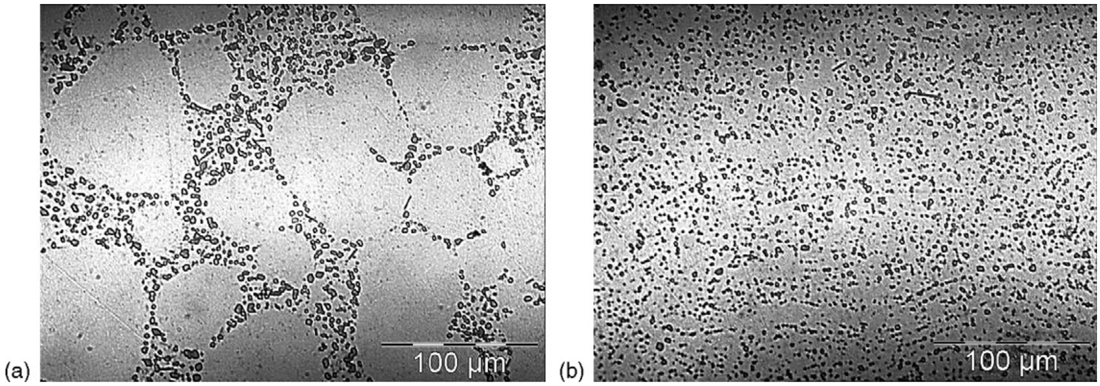

Fig. 6. Microstructure of post HT A356 aluminium: (a) base metal and (b) fusion zone.

higher than that of as cast fusion zone (90 Hv). It was interesting to note that the fusion zone hardness 95 Hv drops to 85 Hv in the overaged HAZ and increases to 125 Hv in the pre HT base metal. The influence of the welding process on the pre HT heat affected zone can be explained by an overaging effect of the fusion heat, which changes the state of coherency of the precipitation to a more non-coherent state. This could be the reason for a drop in the hardness and strength of the metal in the HAZ. The substructure changes are being investigated at the moment and will be reported elsewhere.

In the case of welds in the post HT conditions the weld metal also underwent a heat treatment cycle. The average hardness of base metal, HAZ and fusion zone was 130 Hv. This is also in line with the base metal hardness (125 Hv) of the pre HT outside the HAZ. It was found that the hardness in the fusion zone of post HT was 30% higher than pre HT and as cast conditions. The reason for this is that while the welding process will negate the effect of the pre HT by dissolving the precipitates and post HT will produce precipitation hardening in the weld metal.

There has been a large variation in the hardness of the base metal of as cast material and to some extent also in the fusion zone (Fig. 7). In the base metal, the α-aluminium grain size was 85–95 μm, which was much larger than the indent of the Vickers machine. When the indent fell on an α-aluminium grain, the result was a lower hardness, while when the indent fell on a eutectic, the hardness was higher. However, an intermediate hardness was achieved when it fell on both α-aluminium and eutectic. In the fusion zone, the hardness was more uniform due to the very fine dendrite structure.

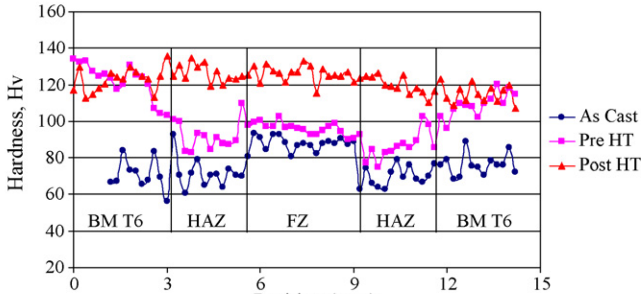

Fig. 7. Micro-hardness of SSM A356 across the weld for as cast, pre HT and post HT samples, FZ (fusion zone), HAZ (heat affected zone) and BM (base metal).

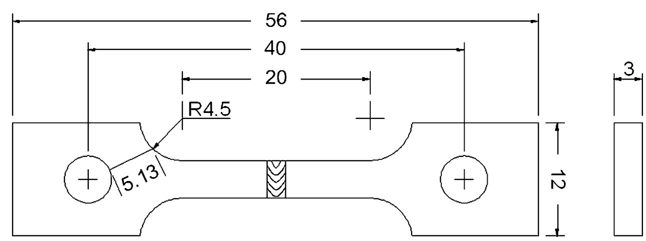

Fig. 8. The tensile test specimen.

4.4. Mechanical properties

The aluminium welding was carried out with the optimal laser welding parameters (Fig. 3), resulting in welds, which were free of cracks and porosities. The welded 4 mm plates were machined down to 3 mm thickness to remove the roots and weld face undercuts. The tensile weld specimens were prepared with the weld in the centre according to the dimension shown in Fig. 8. The measured mechanical properties are averaged value of five samples for F and each HT conditions.

Fig. 9 shows the changes in mechanical properties of A356 in the as cast (F), pre HT and post HT conditions. The mechanical

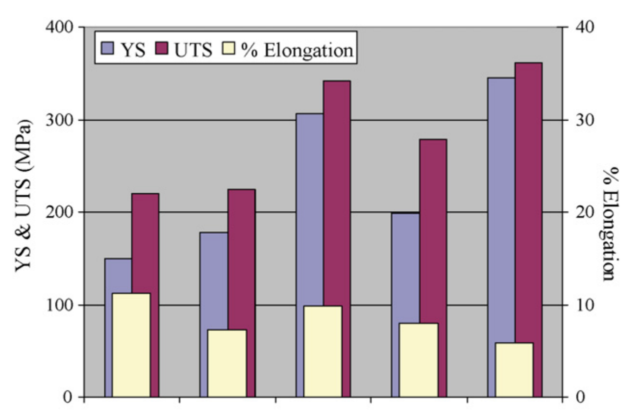

Fig. 9. Yield strength (YS), ultimate tensile strength (UTS) and % elongation of unwelded and welded as cast, pre HT and post HT samples.

properties (yield strength, YS and ultimate tensile strength, UTS) of the as cast welded samples were relatively higher than the as cast unwelded sample, indicating that the weld is stronger than the base metal. The fine dendrite microstructure obtained in the weld metal is normally responsible for the improvement of the mechanical properties. The fracture in tensile test occurred in the base metal.

The mechanical properties of the welded pre HT samples were lower than the unwelded HT samples. The heat treatment of the base metal resulted in the increase of mechanical properties, however, due to the fusion heat during welding the heat affected zone (HAZ) experience an over aging effect and hence a relative drop in mechanical properties. This fact could be explained with the strengthening mechanism during the T6 HT. After aging at 160 °C/6 h of the super saturated solid solution of aluminium coherent particles segregated, giving its maximum strength to the alloy A356. During welding, the fusion heat facilitates the diffusion and the segregation grows, this become less coherent, with a respective drop in the strength and hardness of the metal in the heat affected zone. Due to this effect the fracture in tensile test occurred in the HAZ. However, the YS and UTS of the pre HT welded samples were still higher (200 and 270 MPa, respectively) than the as cast welded and non-heat treated samples (170 MPa/220 MPa) indicating that the pre HT process yield stronger base metal as compared to as cast material. The laser welding process is too quick and is not able to produce enough heat for non-coherent particles segregation and the strength parameters of the alloy to be returned to their as cast condition values.

This process, typical for laser welding could be called as residual strengthening effect of the pre heat treated base metal. A more detailed R&D work is in progress and transmission electron microscopy should be involved and the modification of the aging process to be revealed.

In the case of post heat treated welds, the tensile properties were higher than for the unwelded samples, as opposed to the pre HT samples, indicating that the post HT weld is much stronger than pre HT welded and unwelded samples. The higher tensile strength obtained in the post HT welds is attributed to the change in microstructure as explained in the previous section. Thus it is suggested to perform the weld first in as cast condition and provide the heat treatment after welding to obtain greater strength in both the weld and base metal. In the post HT welds, fracture occurred either at base metal or HAZ. This indicates that weld fusion zone was stronger than the base metal and HAZ.

The elongation in the unwelded samples was higher than welded samples in both the as cast and heat treated samples. The elongation of pre HT sample was higher than the post HT sample, which corresponds to the higher YS & UTS.

5. Conclusions

The microstructure of the as cast base metal consisted of globular primary phase α-Al and a eutectic mixture of Al and Si. The fusion zone consisted of a fine dendrite structure. The microstructure of pre HT base metal consisted of globular primary phase α-Al, but the eutectic phase in the as cast material was converted to spherodized Si particles embedded in α-Al phase. The fusion zone was similar to the as cast weld. The microstructure of post heat treated base metal was same as pre HT base metal however, the fusion zone eutectic was also converted to globular Si particles distributed in Al matrix throughout the weld.

The hardness of the weld metal, in case of the as cast sample was 10–15% higher than the base metal. The hardness of pre HT sample in the fusion zone was slightly higher than as cast fusion zone samples. However, the hardness of the fusion zone (95 Hv) drops to 85 Hv at the HAZ, but increases to 125 Hv in the base metal away from the HAZ, which was not affected by the fusion heat. The average hardness of the post HT sample was almost same (130 Hv) for base metal, HAZ and fusion zone. The hardness of the post HT sample in the fusion zone was 30% higher than as cast and pre HT fusion zone.

The tensile properties (YS & UTS) of pre HT welded samples were lower than the unwelded HT samples. However, the properties of post HT sample were higher than both unwelded and pre HT sample. The elongation of the welded samples in as cast, pre HT and post HT were lower than the unwelded samples indicating a reduction in ductility after welding.

Acknowledgements

The authors are grateful to Mr. Corney van Rooyen and Mr. Patrick Kazadi for helping in the experimental arrangements.

References

[1] H.K. Jung, P.K. Seo, C.G. Kang, J. Mater. Process. Technol. 113 (2001) 568–573.
[2] D. Brabazon, D.J. Browne, A.J. Carr, Mater. Sci. Eng. A 356 (2003) 69–80.
[3] R. Febbro, K. Chouf, J. Laser Appl. 12 (2000) 142–146.
[4] M. von Allmen, Laser Beam Interaction with Metals, Springer-Verlag, Berlin, 1987.
[5] S. Ramasamy, C.E. Albright, J. Laser Appl. 12 (2000) 101.
[6] M.L. Santella, T. Engstrom, D. Storjohann, T.Y. Pan, Scripta Mater. 53 (2005) 201–206.
[7] L. Ivanchev, D. Wilkins, G. Govender, Proceedings of the Eighth International Conference on Semi-solid Processing of Alloys and Composites, Cyprus, September 21–23, 2004.
[8] E. Orgis, A. Wahlen, H. Luchinger, P.J. Uggowitzer, J. Light Metals 2 (2002) 263–269.